EFFECTS OF TURBULENCE INDUCED BY MICRO VORTEX GENERATORS ON SHOCKWAVE – BOUNDARY LAYER INTERACTIONS

Janusz Sznajder, Tomasz Kwiatkowski

Institute of Aviation, Department of Aerodynamics
Krakowska Avenue 110/114, 02-256 Warsaw, Poland
tel.: +48 22 8460011 ext. 492, fax: +48 22 8464432
e-mail: jsznaj@ilot.edu.pl, tomasz.kwiatkowski@ilot.edu.pl

Abstract

Interactions between viscous and transonic effects in air flow around a laminar wing were investigated computationally by means of the solution of unsteady Reynolds-averaged Navier-Stokes Equations. The subject is important from the point of view of applications of Natural Laminar Flow technology in modern, economically efficient passenger aircraft. The research was focused on simulations and analyses of influence of turbulence induced by micro vortex generators on intensity of harmful transonic phenomena like strong shock waves and buffet. Two ways of modelling of the effects of turbulators – the micro vortex generators were taken into consideration. The first way consisted in resolving the shape and inclination angle of the generator in the grid over airfoil and setting the non-slip wall boundary condition on the surface of the generator. The second way, taking advantage of the BAY model of vortex generator, was implemented on orthogonal grid without the need of resolving the shape of the vortex generator in the grid. Calibration of the BAY model was aimed at producing similar distribution of vorticity and velocity circulation behind the model of the vortex generator, as obtained for the grid-resolved model of the vortex generator. The calibration procedure resulted, however, in overestimated turbulisation of the boundary layer in the BAY model, compared to the effects of the grid-resolved vortex generator. The flow simulations indicated, however, that turbulisation of boundary layer induced by micro vortex generators can reduce or eliminate the oscillation of strong shock wave and buffet in off-design conditions and that further adjusting of the BAY model is an efficient strategy for modelling the interactions between viscous and transonic effects in air flow around a laminar wing.

Keywords: transonic flow control, laminar-turbulent transition, vortex generators, flow simulations, BAY method

1. Introduction

Laminar airfoil design is directed towards obtaining as long as possible extent of laminar flow (in practice 50-60% of airfoil chord) in order to achieve low drag values in cruise conditions. In transonic flow, however, when flow over a significant part of the airfoil is supersonic this may lead to laminar shockwave-boundary layer interaction with appearance of a strong shockwave and immediate flow separation and rise of aerodynamic drag. Additionally, strong shockwave may be unstable and oscillate along the chord, which is known as buffet phenomenon. These oscillations cause large-amplitude oscillations of pitching moment which is harmful to wing structure and should be avoided by excluding these dangerous Mach number and angle-of-attack combinations from flight envelope.

Numerical investigations of laminar-turbulent transition and its effects on aerodynamic characteristics of airfoil in transonic flow can be conducted by different methods. The first effective approach involved viscous-inviscid interaction, as e.g. in [3] where computational domain is divided in two zones. In a zone outside boundary layer where viscous effects can be neglected, full-potential equations are being solved and in a viscous zone close to airfoil surface integral boundary layer equations, obtained from Prandtl boundary layer equations are solved. On the outer edge of the boundary layer, iterative aligning of tangential velocities obtained from inviscid flow solution and from the solution of boundary layer equations is conducted. The

advantage of this approach is relatively low cost of the solution because of avoiding the need to solve Navier-Stokes equations with larger number of variables. The drawback of this approach is that the thickness of boundary layer is modelled by artificial quantity – transpiration velocity and the velocities in the boundary layer are not computed directly for given boundary conditions but result from streamwise integration of boundary layer equations and iterative aligning with external flow. This limits the applicability of this approach to flows with low three-dimensional effects and makes it unsuitable for analysing effects of flow-control devices, such as micro-vortex generators placed in the boundary layer. More of physical phenomena in the boundary layer can be accounted for by solution of Unsteady Navier-Stokes equations (URANS) with turbulence models resolving transitional flow. The four-equation Transition SST turbulence model of ANSYS Fluent where transport equations are applied for turbulent kinetic energy, turbulence dissipation rate, intermittency and laminar-turbulent transition onset criteria, based on γ-Re_θ model, [2] allows for simulation of transitional flows and analysis of interactions between laminar, turbulent and transitional flows in the boundary layer with shock-waves.

In the European 7-th Frame Work Programme Project TFAST the effects of transition location on the structure of shock wave/boundary layer interactions are studied both experimentally and by numerical flow simulations. This includes the effects of enforcing laminar to turbulent transition in different locations in order to obtain low-drag laminar fragment of the flow and turbulent boundary layer/shock wave interaction. In the presented work flow around V2C laminar airfoil designed by Dassault Aviation is investigated. In the investigated conditions of free-stream (Mach Number equal to 0.7, Reynolds Number equal 3.42 million, and angle of attack α equal to 4) there occurs strong oscillating shock wave with flow separation behind the shock wave. In order to alleviate the unfavourable flow phenomena turbulisation of the boundary layer is induced by delta-shaped, micro-vortex generators located in the laminar boundary layer ahead of the shock. In the presented work vortex, generators were modelled by resolving their shape and inclination in the computational grid, as well as in an alternative way, using the BAY method, which introduces momentum sources in high-quality orthogonal mesh without local deformations of the grid cells.

2. Analysed configurations

Flow simulations were conducted for three configurations: the baseline configuration of clean constant-chord wing strip and two configurations with delta-shaped micro-vortex generator located in the 20% and 50% chord respectively, on the upper wing surface. The wing strip chord was equal to 20 cm. In agreement with the research, methodology assumed in the TFAST projects all configurations included solid upper and lower walls of wind-tunnel test section of the height of 60 cm. The analysed wing strip had width allowing for resolving in the grid one vortex generator of 1 mm length, inclined to the flow at an angle $\beta = 14°$ separated by spaces of 5% of the length of projection of the generator on the plane perpendicular to flow from the lateral sides of the computational domain. (Fig. 1). On the lateral sides of the computational domain, boundary conditions of symmetry were applied. In the front of the computational domain, pressure far-field boundary condition was used and the pressure outlet boundary condition was used in the plane closing the computational domain behind the model. The delta-shaped vortex generator had maximum height of 0.1 mm and wedge angle of 6°.

3. Flow simulation method

For the numerical flow simulation, the ANSYS FLUENT v14.5 three-dimensional, unsteady flow solver was applied. Second-order spatial and temporal discretisation was applied. Pressure-velocity coupled solver was used. The four-equation Transition SST turbulence model, implemented in the FLUENT solver was applied in order to resolve the laminar-turbulent

transition. One way of modelling of vortex generators consisted in application of the BAY method, developed by Bender et al. [1]. In this method, the vortex generator (VG) is replaced by a sub-domain of cells placed in original location of vortex generator, where the force distribution acting on fluid, replicating the effects of a real vortex generator is applied. The force is introduced by a source term on the right-hand side of momentum and energy conservation equations. The force acting on fluid is equal to the side force, proportional to the angle of inclination of the VG with respect to local flow:

$$\vec{L} = c_{\mathrm{VG}} S_{\mathrm{VG}} \frac{\Delta V_i}{V_m} \beta \rho u^2 \vec{l},$$ (1)

where:
$\vec{L}$ – a side force produced by the VG,
c_{VG} – a relaxation parameter which controls the strength of the side force,
S_{VG} – the area of VG,
ΔV_i – volume of the cell where the force is calculated,
V_m – the sum of volumes of cells where the force term is applied,
β – the angle of local velocity $\vec{u}$ to the VG,
$\vec{l}$ – unit vector on which the side force acts.

Geometry of the VG is shown in Fig. 1. In the current implementation of the BAY method the side forces are introduced as source terms into the right-hand sides of the momentum conservation equations by the User Defined Functions available in ANSYS FLUENT v14.5 into orthogonal cells surrounding the contour of the VG shown in Fig. 2.
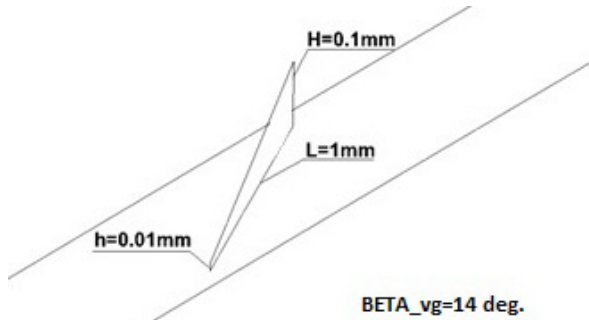

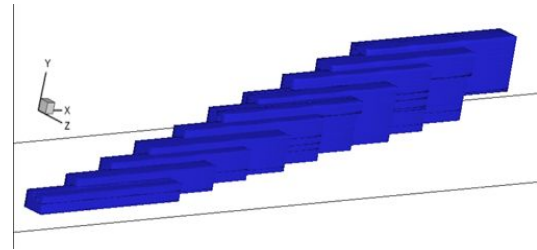*Fig. 1. Geometry of the delta-shaped vortex generator*

Fig. 2. Cells, where momentum source is applied

3.1. Reference flow conditions

The reference flow conditions in all presented flow simulations were as follows: Free stream Mach number: $Ma = 0.70$, airfoil angle of attack: $\alpha = 4°$, airfoil chord: 0.2 m, Reynolds number: 3.42 million, free-stream intermittency: $I = 1$.

4. Results of flow simulations

4.1. Calibration of the BAY model of vortex generator

Current implementation of the BAY method allows for modification of the lateral force produced by the BAY model of a VG by modification of the constant c_{VG} in Eq. (1). The constant has been chosen so as to replicate as closely as possible distribution of X-component of vorticity $\vec{\omega} = \vec{\nabla} \times \vec{V}$ in control planes normal to airfoil surface behind the VG and to match the chordwise profile of vortex circulation Γ defined by Eq. (2) obtained from model resolving exact shape of vortex generators in the grid.

$$\Gamma = \iint_S (\vec{\nabla} \times \vec{V})\,\mathrm{d}S. \tag{2}$$

A close match of the distribution of vorticity in the control planes and chordwise distribution of circulation Γ behind the generator was obtained for $c_{VG} = 2000$. The results of the procedure conducted for the VG located at 20% wing model chord are shown in Fig. 3 and 4.
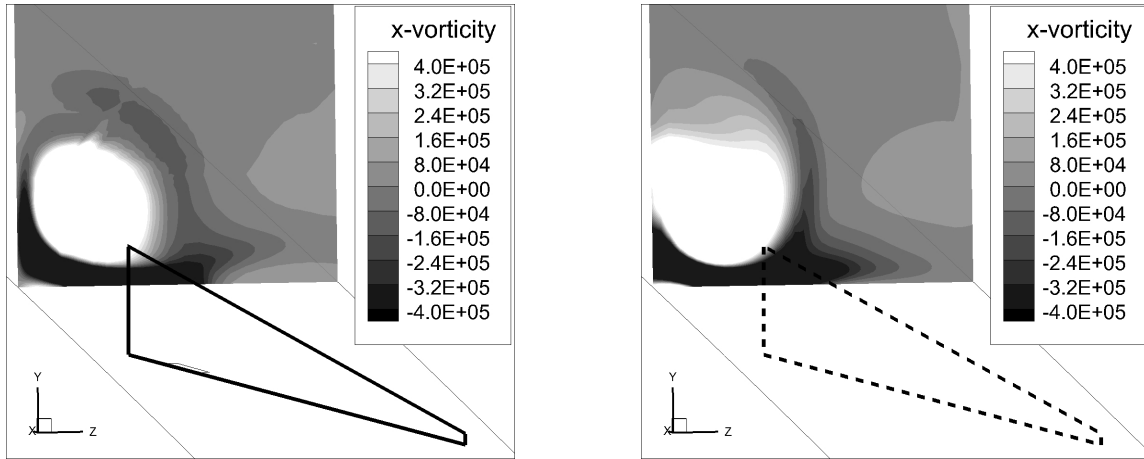

Fig. 3. Distribution of X-vorticity in a control plane located at $(x–xt)/h = 0.15$ downstream of the grid-resolved vortex generator (left) and BAY-modeled vortex generator (right)
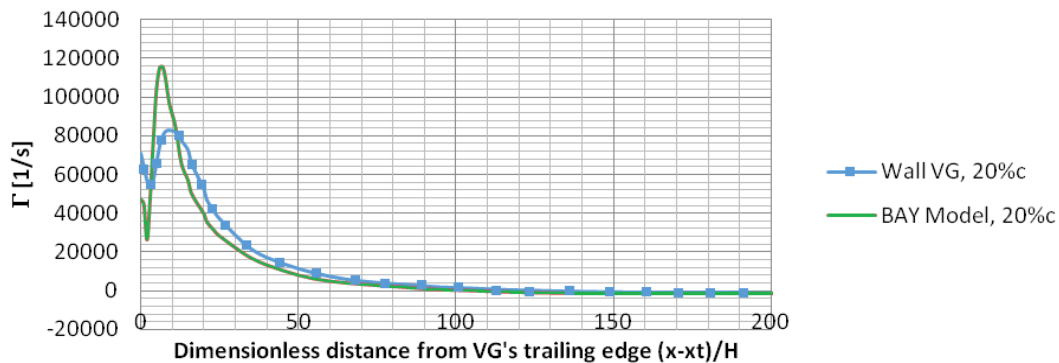
Fig. 4. Decay of velocity circulation produced by grid-resolved vortex generator and the BAY model of the generator

The iterative procedure of modification of the c_{VG} constant produced a chordwise distribution of velocity circulation which is first lower than circulation produced by the grid-resolved VG, then after distance of four VG heights exceeds it and further downstream, after 11 generator heights is slightly underestimated in comparison to the circulation generated by the grid-resolved VG. It is possible that application of a denser grid in the zone surrounding the generator could produce closer match between the results for grid-resolved and BAY-modelled VGs.

4.2. Interactions of shock wave with boundary layer

In the reference flow conditions the flow around the baseline configuration is characterized by oscillating shock wave with oscillation of approximately 80 Hz and amplitude equal to approximately 0.1 chord. The computed pressure distributions in extreme frontal and rear shock positions are shown in Fig. 5. In parallel with the flow simulations, experimental investigations of the airfoil characteristics were conducted at the transonic wind tunnel of the Institute of Aviation. Due to constraints in the frequency of pressure measurements, only the time-averaged pressure distributions over the airfoil surface could be measured. The comparison of the computed pressure distribution, averaged over one oscillation cycle and of the experimentally measured pressure
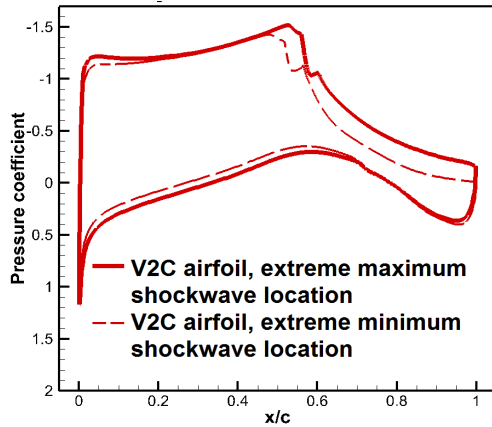
Fig. 5. Pressure coefficient distributions for extreme shock positions of the baseline V2C airfoil
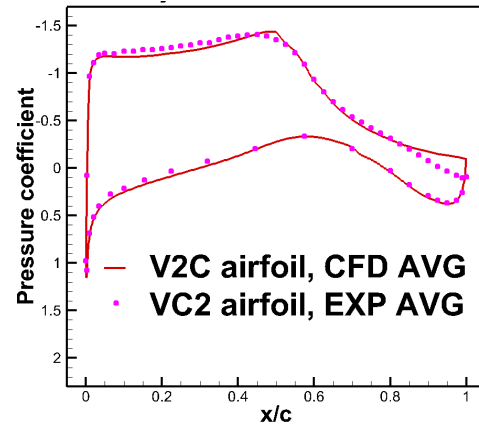

Fig. 6. Comparison of the computed (red line) and experimentally measured (blue, dashed line), averaged pressure distributions over the V2C airfoil

distribution over the baseline V2C airfoil, averaged over time of 2 seconds with the frequency of 333 Hz. is presented in Fig. 6.

The comparison of the computed and the measured averaged pressure coefficient distribution over the baseline airfoil, especially in the region of the shock wave oscillations indicates indirectly, by the similar slope of the curve fragments, that the computed amplitude of the shock wave oscillations presented in Fig. 5 is well predicted. The numerical solution indicates separated flow in trailing-edge region. Positive value of the pressure coefficient in the experimentally measured pressure distribution near the trailing edge may indicate that flow separation does not occur in this region.

4.3. Vortex generator placed in 20% chord

Computed distributions of pressure coefficient for the configuration with VG located in 20% chord are shown in Fig. 7. The small peak at $x/c = 0.2$ in upper-surface pressure-coefficient distribution is caused by pressure jump produced by the VG. Three other small peaks result from grid distortions in locations where model of grid-resolved VG can be implemented by change of boundary conditions from "interior" to "wall" on dedicated grid planes. The grid-resolved model of the VG predicts reduction of the amplitude of shockwave oscillations approximately by 50%. In the case of BAY-modeled VG the amplitude of oscillations is reduced to zero. Clues for the reasons of this difference may be drawn from the comparison of the intermittency, which is a measure of turbulisation of the boundary layer computed for the two models of VGs. By comparison of the data presented in Fig. 8 and 4 it can be seen, that in spite of faster decay of circulation predicted by BAY model than by grid-resolved model of the VG, the intermittency produced by the BAY model is higher than intermittency produced by the grid-resolved model of VG. In the configuration with the BAY model the boundary layer reaching the shock wave is fully turbulent whereas lower than one value of intermittency produced by the grid-resolved model indicates transitional flow. In Fig. 9 comparison of the x-wall shear stress, $\tau_{xx} = \partial u/\partial x$ for the analysed configurations is presented. The results for the baseline, clean configuration predict low value of τ_{xx}, consistent with the laminar character of flow until reaching the shock wave and subsequent flow separation in the zone behind the shock wave until the trailing edge. For the cases with models of the VG there occurs an increase of τ_{xx} behind the VG with the values predicted for the BAY model exceeding those for the grid-resolved model. For both cases of models of VGs the flow is separated overall distance from the shock wave to the trailing edge, just as for the baseline configuration. The small peaks of τ_{xx} in the plot for grid resolved VG are due to local cell deformations, just as explained before, for Fig. 7.
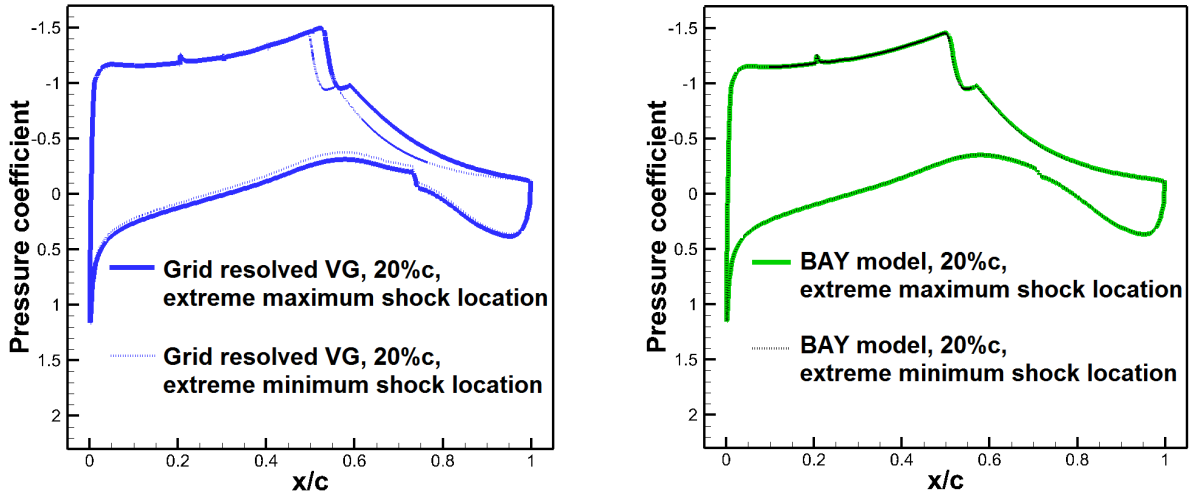
Fig. 7. *Comparison of distributions of pressure coefficient in extreme shockwave locations computed for configuration with vortex generator located in 20% chord for grid-resolved model (left) and for BAY model of vortex generator (right-curves overlapping).*
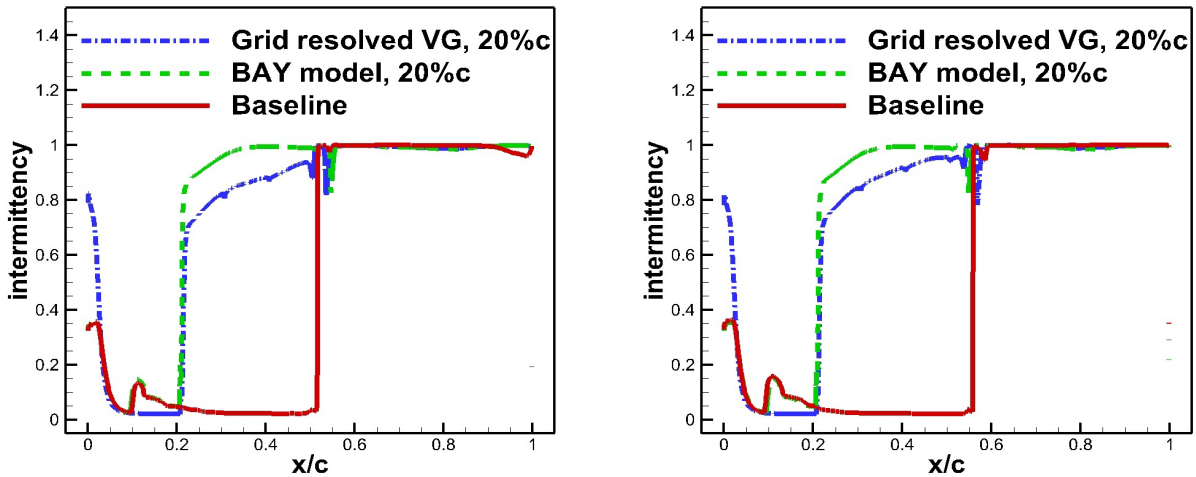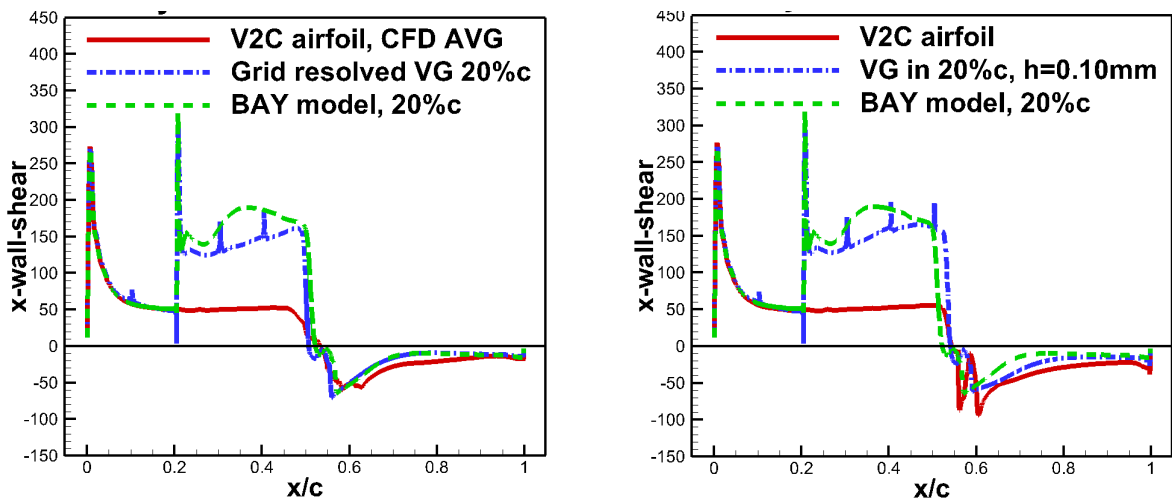

Fig. 8. *Comparison of chordwise distributions of intermittency computed at the height of top vertex of the vortex generator in extreme shockwave locations for the baseline configuration and for two configurations with models of the vortex generator at 20% chord.*

Fig. 9. *Comparison of chordwise distributions of X-component of wall shear stress computed at the height of top vertex of the vortex generator in extreme shockwave locations for the baseline configuration and for two configurations with models of the vortex generator at 20% chord*

4.4. Vortex generator placed in 50% chord

Similar analysis of interactions of boundary layer flow with shock wave was conducted for VG placed in 50% chord. The height of the VG was the same – 0.1 mm. As can be seen in Fig. 10, the model of grid-resolved VG did not reduce the amplitude of oscillations of the shock wave, which remained close to 10% of airfoil chord. In contrast, the results of the BAY model show significant reduction of the amplitude of oscillations of the shock wave, limiting its movement to the zone behind the generator. As in the case of VG placed in 20% chord this reduction of amplitude of shockwave oscillations can be traced to over predicting of turbulence level by the BAY model, which is visible in the intermittency plots in Fig. 11. The character of changes of τ_{xx} shear stress for the baseline case and for the cases with modelled vortex generator is also similar to the changes for VG located at 20% chord.
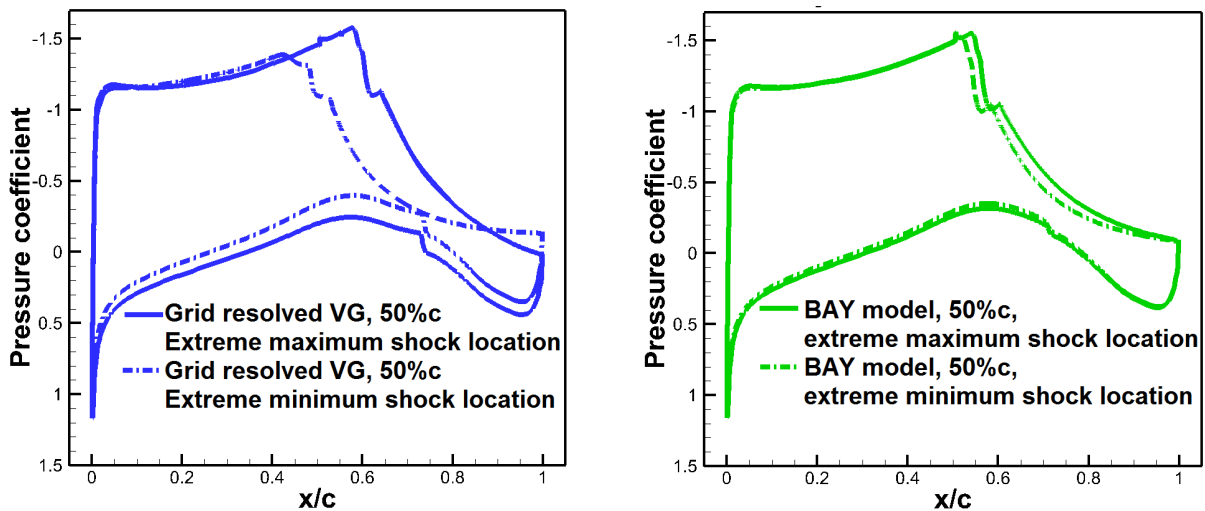

Fig. 10. Extreme shock-wave positions predicted by the grid-resolved and BAY model of a 0.1 mm-high vortex generator located in 50% chord
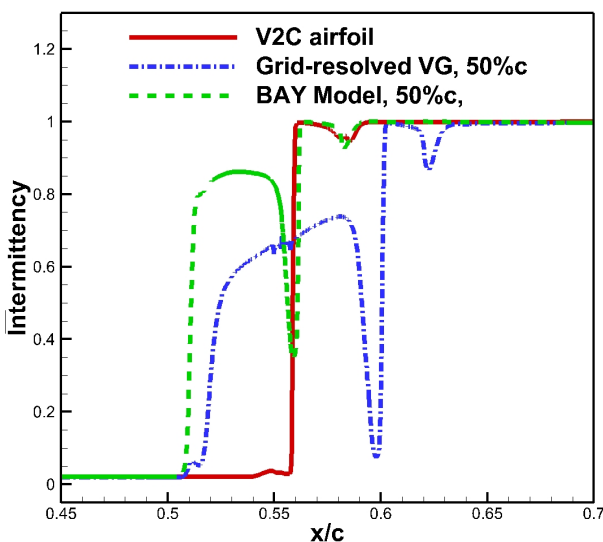

Fig. 11. Comparison of chordwise upper-surface distributions of intermittency computed at the height of top vertex of the vortex generator for the baseline configuration and for two configurations with models of the vortex generator at 50% chord at the shock rear extreme position
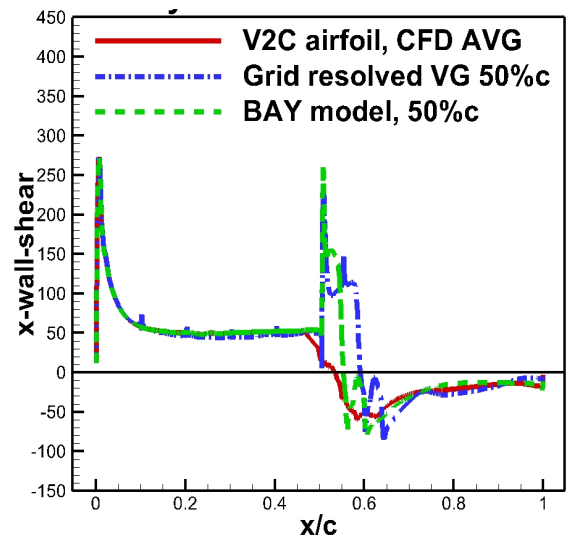
Fig. 12. Comparison of chordwise distributions of X-component of wall shear stress computed at the height of top vertex of the vortex generator in extreme rear shock locations for the baseline configuration and for two configurations with models of the vortex generator at 50% chord

5. Conclusions and future work

Calibration of the BAY model was aimed at obtaining good matching of distributions of the X-component of vorticity in the selected cross sections behind the vortex generator and similar profile of decay of the velocity circulation behind the BAY-model of the generator, compared to the grid-resolved vortex generator. This procedure resulted, however, in higher peak value of velocity circulation behind the vortex generator than produced by the grid-resolved vortex generator and also in overestimated values of intermittency in the zone behind the vortex generator. This means that the turbulisation effects in the boundary layer obtained with the BAY model of vortex generator were stronger than the effects of the grid-resolved vortex generator. The higher turbulisation predicted by the BAY model stabilised the shock-wave in stationary position for the model of vortex generator located in 20% of chord and significantly reduced the amplitude of shock-wave oscillations for the model of vortex generator located in 50% of airfoil chord. This, considering also the lower than unity values of intermittency produced by the 0.1 mm-high grid resolved vortex generators leads to the conclusion that a proper location and a proper height of a vortex generator can be found, that can stabilise the position of the shock-wave in off-design conditions, reducing or eliminating the buffet oscillations of shockwave. This solution can become a realizable technological device, deployable or fixed. The future work will concentrate on finding more effective shape and position of the vortex generator and concentrate on more precise calibration of the BAY model in order to model the effects of vortex generators on shock wave – boundary layer interactions more closely.

Acknowledgements

References

[1] Bender, E. E., Anderson B. H., Yagle, P. J., *Vortex generator modelling for Navier-Stokes codes*, American Society for Mechanical Engineers, FEDSM 99-6919, New York 1999.

[2] Langtry, R. B., Menter, F. R., *Transition modeling for general CFD applications in aeronautics*, AIAA 2005-522, 2005.

[3] Rokicki, J., Stalewski, W., Żółtak, J., *Evolutionary methods for design, optimization and control*, eds: T. Burczynski and J. Périaux, CIMNE, Barcelona, Spain 2009.